World Academy of Science, Engineering and Technology
International Journal of Chemical and Molecular Engineering
Vol:11, No:8, 2017

Preparation of Fe, Cr Codoped TiO_2 Nanostructure for Phenol Removal from Wastewaters

N. Nowzari-Dalini, S. Sabbaghi

***Abstract*—**Phenol is a hazardous material found in many industrial wastewaters. Photocatalytic degradation and furthermore catalyst doping are promising techniques in purpose of effective phenol removal, which have been studied comprehensively in this decade. In this study, Fe, Cr codoped TiO_2 were prepared by sol-gel method, and its photocatalytic activity was investigated through degradation of phenol under visible light. The catalyst was characterized by XRD, SEM, FT-IR, BET, and EDX. The results showed that nanoparticles possess anatase phase, and the average size of nanoparticles was about 21 nm. Also, photocatalyst has significant surface area. Effect of experimental parameters such as pH, irradiation time, pollutant concentration, and catalyst concentration were investigated by using Design-Expert® software. 98% of phenol degradation was achieved after 6h of irradiation.

***Keywords*—**Wastewater, doping, metals, sol-gel, titanium dioxide.

I. Introduction

In recent years, photocatalysts have been extensively investigated. Photocatalysts are utilized in many applications such as hydrogen production, solar cells, and wastewater treatment. TiO_2 gained the main focus because of its properties: non-toxicity, low cost, and chemical stability. However, large band gap of TiO_2 (3.0-3.2 eV) causes TiO_2 to show photocatalytic activity under ultraviolet (UV) irradiation. A wide range of effort has been made to extend the spectral response of TiO_2 to visible light by metal or non-metal doping. Doping can be achieved by various methods like sol-gel method, hydrothermal method, and wet-impregnation method. Akpan and Hameed stated the advancement in sol-gel method [1]. Sol-gel, modified sol-gel, and other kinds of sol-gel processes were investigated along with single, nonmetal, metal and codoping of titanium dioxide. In most cases of codoping, especially when one element is metal, photocatalytic activity is improved [2]. Kerkez-Kuyumcu et al. investigated a comparative study of the doping of six successive transition metal elements for removal of dyes under visible light [3]. Photocatalyst was prepared by modified precipitation method. Cu/TiO_2 showed highest photocatalytic activity under visible light among the other transition metals. Liu et al. reported synthesis of Fe, N, codoped TiO_2 through hydrothermal method [4]. Photocatalytic activity was examined through degradation of methylene blue solution under visible light. In the present study, sol-gel method was used to synthesize Fe, Cr codoped TiO_2. Then, it was subjected to several characterization methods.

S. Sabbaghi is with the Shiraz University, Faculty of Advanced Technologies, NanoChemical Eng. Dept., Shiraz, Iran (phone: +989171133471; fax: +9871-36139669; e-mail: sabbaghi@ shirazu.ac.ir).

N. Nowzari-Dalini is with the Shiraz University, Faculty of Advanced Technologies, NanoChemical Eng. Dept., Shiraz, Iran (e-mail: nz.nowzari@gmail.com).

II. Photocatalyst Synthesis

A. Experimental

Titanium isopropoxide (TTIP), nitric acid, ethanol, $Cr(NO_3)_3.9H_2O$, and $Fe(NO_3)_3.9H_2O$ were procured from Merck® and were used without further purification. Initially, 5 ml of TTIP was mixed with 50 ml ethanol under magnetic stirring at room temperature. Then, appropriate amount of metal precursor was added to the solution while vigorous stirring. Finally, greenish gel was resulted shortly after 5 ml of nitric acid was added. The resulting gel was dried in room temperature for three days then was calcinated at 400 °C for 4 h to give TiO_2 powder. Single and codoping TiO_2 nanoparticles were synthesized using almost the same method. The appropriate amount of $Fe(NO_3)_3•9H_2O$ or/and $Cr(NO_3)_3•6H_2O$ was calculated from desired molar ratio of Fe/Ti=0.01 and Cr/Ti=0.005 and then dissolved in anhydrous ethanol, which was added to the distilled water prior to the hydrolysis of TTIP.

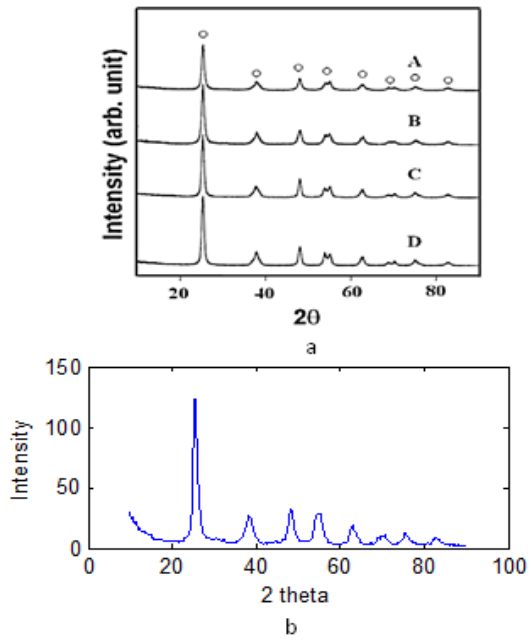

Fig. 1 XRD pattern of Fe/Cr codoped TiO_2 :(a) XRD patterns of materials: (A) Cr-doped TiO_2 (B) Fe-doped TiO_2 (C) Fe and Cr codoped TiO_2 (D)TiO_2 calcinated at 400 °C. O: Anantase phase [5] (b) Current study XRD pattern of Fe/Cr codoped TiO_2

B. Characterization

The phase compositions of samples were determined by a D8 ADVANCE X-ray diffractometer (XRD) equipped with graphite monochromatized Cu Kα radiation. The morphology of the sample was observed by using scanning electron microscopy (VEGA3 SB – EasyProbe) along with EDX. FT-IR analysis was operated by PerkinElmer FT-IR with the model of Spectrum RXI. BET surface area, total pore volume, and the pore size volume of the catalysts were measured by N_2 physisorption at 77.26 K using Micromeritics ASAP 2020 V3.03 system.

XRD patterns of codoped TiO_2 are shown in Fig. 1. The distinct peaks of anatase phase of TiO_2 is demonstrated in Fig. 1 (a) and compared to current study XRD pattern (shown in Fig. 1 (b)) confirms formation of anatase TiO_2.

FT-IR spectrum of codoped TiO_2 is given Fig. 2. A broadband can be seen in the 400-900 cm^{-1} region which is attributed to Ti-O-Ti bond of anatase titania [4]. Peaks at 3400 and 1600 cm^{-1} represents the O-H vibrational bond and water absorption respectively [6].

Fig. 3 shows the SEM results of mentioned catalyst. It can be figured from the photo that particle size varies between 16-29 nm, and the estimated average size is 21 nm. Elemental compositions of codoped TiO_2 can be determined from EDX diagram which are shown in Table I. Results show that they are in good agreement with theoretical calculations.

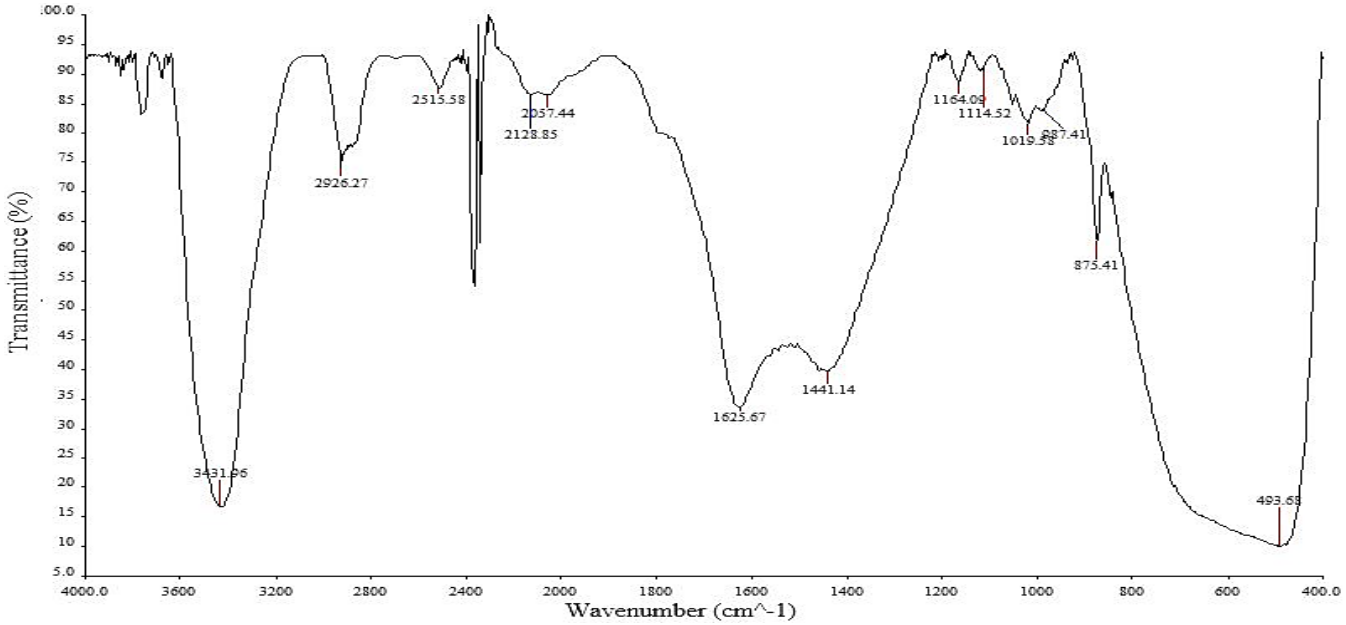

Fig. 2 FT-IR spectra of codoped TiO_2

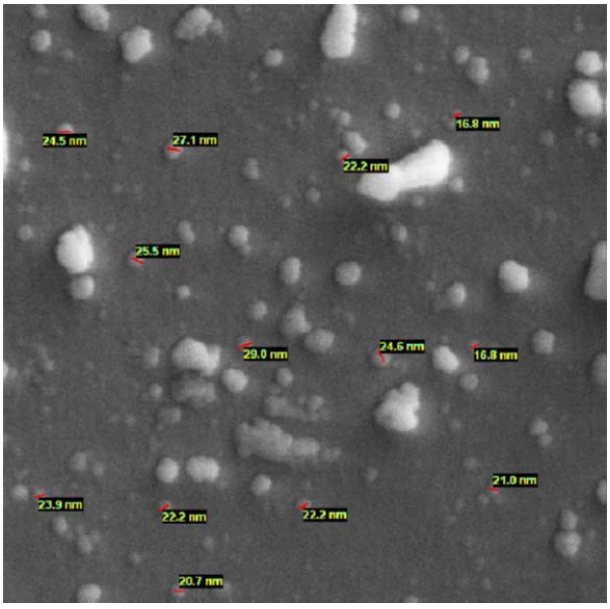

Fig. 3 SEM images of codoped TiO_2

TABLE I
COMPOSITIONS OF CODOPED TIO_2

Element	Line	Intensity (keV)	Weight percent (%)
C	Ka	1.5	2.95
O	Ka	4.6	13.84
Ti	Ka	51.7	74.94
Cr	Ka	0.9	2.33
Fe	Ka	1.1	5.95

The textural properties of catalysts were determined through BET measurements such as surface area, pore size distribution and total pore volume. The results are listed in Table II.

Results shows sol-gel synthesized Fe, Cr codoped TiO_2 has higher total surface area than hydrothermal synthesized ones [5],[7]. Also, total pore volume and average pore diameter have improved.

TABLE II
RESULTS OF BET ANALYSIS

Photocatalyst	Total surface area (m^2/g)	Total pore volume (cm^3/g)	Average pore diameter (A)
Fe, Cr codoped TiO_2	101	0.185	73.42

III. DETERMINATION OF PHOTOCATALYTIC DEGRADATION

Photocatalytic activity was evaluated by degradation of phenol in aqueous solutions with dispersed codoped TiO_2 powders. The photoreaction was conducted in a 150-mL cylindrical vessel above a magnetic stirrer. A 35-W Xenon lamp was located above the vessel. Before irradiation, the suspension was stirred for 30 min in the dark to obtain equilibrium. Permanent air bubbling (rate of 3.5 lit/min) was applied during irradiation in order to keep the concentration of the dissolved oxygen constant. Aliquots of suspension were withdrawn at specified times then centrifuged at 5300 rpm for 30 min. The residual concentration of phenol was analyzed with a Fluorescence Spectrophotometer.

In this study, Design-Expert® software (Ver. 10) was utilized to design the experiments. The ranges and levels of independent variables are shown in Table III. The detailed the designed experiments along with experimental and predicted values of the response are given in Table IV.

TABLE III
THE LEVELS AND RANGES OF VARIABLES IN CCD EXPERIMENT DESIGN

	Name	Units	-1 level	+1 level	-alpha	+alpha
A	pH		5	9	3	11
B	Time	h	2.25	4.75	1	6
C	Catalyst concentration	g/lit	0.4	1	0.1	1.3
D	Phenol concentration	ppm	30	70	10	90

IV. RESULTS AND DISCUSSION

A. Effect of pH

According to results of ANOVA, pH is the second most important parameter in phenol degradation as shown in Fig. 4 (a). It indicates that with increasing of pH, the rate of phenol degradation also increases. Degradation of phenol has been found to be insignificant at low pH values. This phenomenon is due to high concentration of hydroxide in alkaline solutions, which means there is more OH- to react with phenyl ring [8].

B. Effect to Time

As it is shown in Fig. 4 (b), phenol degradation rate increased with time. 98% removal is achieved in 6 h. Also, the highest degradation rate took place in the first 4 h of reaction. After that, rate decreased to become constant after 6 h [9].

C. Effect of Catalyst Concentration

Fig. 4 (c) demonstrates a maximum peak. In the other words, in the ascending section, increasing the amount of catalyst leads to the increase in the surfaces on which phenol can be adsorbed. Meanwhile, in the descending part, when the amount of the catalyst increases, phenol degradation rate decreases. This phenomenon can be attributed from screening effect [10]. After a certain amount, the solution will become opaque, so the contaminant will receive less intensity of light.

TABLE IV
CCD EXPERIMENTS ALONG WITH ACTUAL VALUES OF RESPONSE

No. of experiment	pH	Time (hr)	Catalyst concentration (g/lit)	Phenol concentration (ppm)	Phenol Degradation under visible light (%)
1	7	3.50	0.70	50	33.17
2	9	2.25	0.40	70	24.34
3	9	4.75	0.40	70	49.73
4	7	6.00	0.70	50	56.59
5	5	4.75	1.00	30	34.67
6	7	3.50	0.70	50	33.42
7	5	2.25	0.40	30	17.98
8	5	2.25	0.40	70	13.85
9	9	4.75	0.40	30	69.89
10	9	4.75	1.00	70	51.66
11	7	3.50	1.30	50	26.41
12	7	3.50	0.70	50	33.86
13	3	3.50	0.70	50	13.02
14	5	2.25	1.00	70	22.79
15	5	4.75	0.40	30	41.23
16	9	2.25	1.00	30	24.40
17	7	3.50	0.70	10	69.05
18	7	3.50	0.10	50	11.83
19	5	4.75	0.40	70	34.66
20	7	3.50	0.70	50	34.27
21	7	3.50	0.70	50	34.70
22	7	3.50	0.70	90	35.86
23	9	2.25	1.00	70	32.33
24	5	2.25	1.00	30	15.15
25	9	2.25	0.40	30	34.19
26	7	3.50	0.70	50	35.09
27	11	3.50	0.70	50	62.73
28	5	4.75	1.00	70	38.80
29	7	1.00	0.70	50	11.72
30	9	4.75	1.00	30	52.83

D. Effect of Initial Phenol Composition

Fig. 4 (d) indicates that phenol degradation vs initial phenol composition has a descending trend. With increasing organic contaminant but keeping the catalyst constant, it hinders them to adsorb on TiO_2 surface resulting in lower degradation rate [11].

E. Modeling Removal Rate of Phenol

Design-Expert® based on the results of experiments, shown in Table IV, models the removal rate of phenol. Hence, for modeling, Response Surface method was used, and Central Composite design was chosen. The equation, to show relations between dependent parameter (percent removal of phenol) and other parameters, which was obtained using quadratic model. is shown in (1):

$$Removal = 34.72 + 9.15A + 11.59B + 0.66C - 3.69D + 1.83AB - 1.59BD + 3.7CD - 3.99C^2 + 4.35D^2$$

where A, B, C, and D are the coded values of experimental parameters pH, irradiation time (h), catalyst concentration or

C_0 (gr/lit), and phenol composition (ppm). R-squared of 0.9165 indicates that the model is in good compatibility of the results.

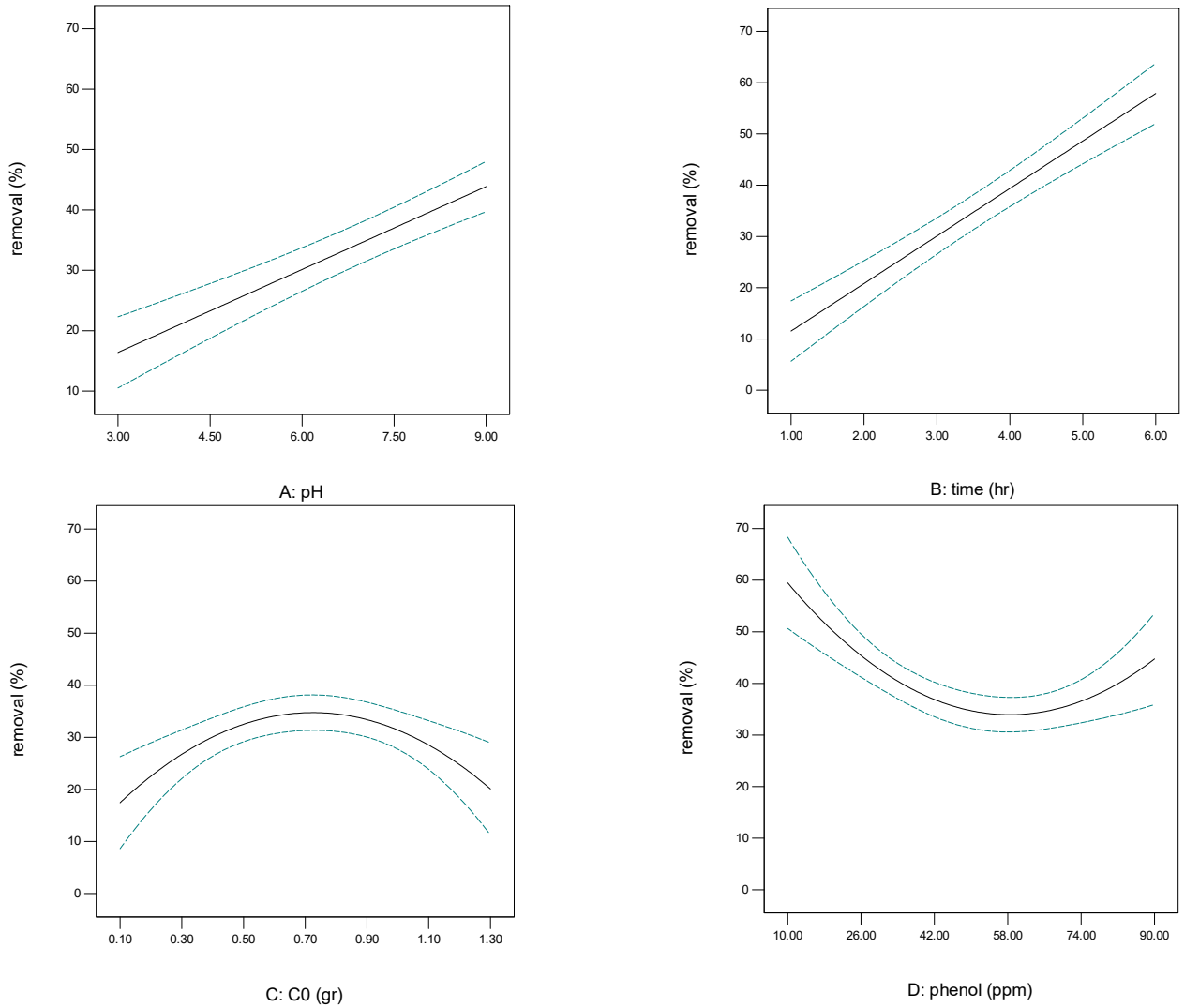

Fig. 4 Percent removal of phenol in respect of parameters. (a) Percent removal of phenol with respect to pH at constant condition of time=3.5h, C_0=0.7 gr/lit and phenol concentration=50 ppm. (b) Percent removal of phenol with respect to time at constant condition of pH=7, C_0=0.7 gr/lit, and phenol concentration=50 ppm (c) Percent removal of phenol with respect to C_0 at constant condition of pH=7, time=3.5h, and phenol concentration=50 ppm (d) Percent removal of phenol with respect to phenol concentration at constant condition of pH=7, time=3.5h, and C_0=0.7 g/lit

TABLE V
OPTIMAL CONDITION

Effective parameters	Optimal value
pH	11
Irradiation time (h)	6
Catalyst concentration (gr/lit)	1
Phenol concentration (ppm)	10

TABLE VI
COMPARATIVE RESULTS OF PHENOL REMOVAL STUDIES

Type of process	Irradiation time (h)	Phenol concentration (ppm)	Phenol degradation (%)	Researchers
N TiO_2 + Xe	1	100	18	[12]
CuO/ZnO/TiO_2 + UV	90	50	75	[13]
Fe TiO_2 + solar light	3	1.88	80	[14]
Cu TiO_2	3	158.75	52	[15]
Fe/Cr TiO_2 + Xe	6	90	98%	This study

F. Optimal Condition

Design-Expert® can estimate the optimal condition based on the given results, which is shown in Table V. 98% of phenol removal can be achieved in this condition.

Table VI shows comparative results of works of researchers with this study. Results show that this method is more efficient in time and catalyst consumption, besides the enhancement of the phenol degradation.

V. Conclusion

In this study, phenol degradation from wastewater using Fe/Cr codoped TiO_2 was investigated. It can be concluded from the experiments that codoping of titania increases photocatalytic activity meaning that iron and chromium are good dopants due to their similar radius to titanium [16]. Furthermore, alkaline environment, suitable concentration of catalyst, and longer irradiation time can help to increase the removal rate. In optimal condition, phenol can be removed completely.

References

[1] Akpan, U. and B. Hameed, *The advancements in sol–gel method of doped-TiO 2 photocatalysts.* Applied Catalysis A: General, 2010. 375(1): p. 1-11.

[2] Yuan, Z.-h., J.-h. Jia, and L.-d. Zhang, *Influence of co-doping of Zn(II)+Fe(III) on the photocatalytic activity of TiO2 for phenol degradation.* Materials Chemistry and Physics, 2002. 73(2–3): p. 323-326.

[3] Kerkez-Kuyumcu, Ö., et al., *A comparative study for removal of different dyes over M/TiO 2 (M= Cu, Ni, Co, Fe, Mn and Cr) photocatalysts under visible light irradiation.* Journal of Photochemistry and Photobiology A: Chemistry, 2015. 311: p. 176-185.

[4] Liu, Z., et al., *Characteristics of doped TiO2 photocatalysts for the degradation of methylene blue waste water under visible light.* Journal of Alloys and Compounds, 2010. 501(1): p. 54-59.

[5] Jeong, E., et al., *Hydrothermal synthesis of Cr and Fe codoped TiO2 nanoparticle photocatalyst.* Journal of Ceramic Processing Research, 2008. 9(3): p. 250-253.

[6] George, S., *Infreared and Raman Characteristic Group Frequencies*. 2001.

[7] Hussain, S.T. and A. Siddiqa, *Iron and chromium doped titanium dioxide nanotubes for the degradation of environmental and industrial pollutants.* International Journal of Environmental Science & Technology, 2011. 8(2): p. 351-362.

[8] Bubacz, K., et al., *Methylene blue and phenol photocatalytic degradation on nanoparticles of anatase TiO2.* Polish Journal of Environmental Studies, 2010. 19(4): p. 685.

[9] Hayat, K., et al., *Nano ZnO synthesis by modified sol gel method and its application in heterogeneous photocatalytic removal of phenol from water.* Applied Catalysis A: General, 2011. 393(1): p. 122-129.

[10] Siddiqa, A., et al., *Cobalt and sulfur codoped nano-size TiO2 for photodegradation of various dyes and phenol.* Journal of Environmental Sciences, 2015. 37: p. 100-109.

[11] Chiou, C.-H., C.-Y. Wu, and R.-S. Juang, *Photocatalytic degradation of phenol and m-nitrophenol using irradiated TiO 2 in aqueous solutions.* Separation and Purification Technology, 2008. 62(3): p. 559-564.

[12] Peng, F., et al., *Synthesis and characterization of substitutional and interstitial nitrogen-doped titanium dioxides with visible light photocatalytic activity.* Journal of Solid State Chemistry, 2008. 181(1): p. 130-136.

[13] Mohammadi, M., et al., *Preparation and characterization of TiO2/ZnO/CuO nanocomposite and application for phenol removal from wastewaters.* Desalination and Water Treatment, 2014: p. 1-11.

[14] Nahar, M.S., K. Hasegawa, and S. Kagaya, *Photocatalytic degradation of phenol by visible light-responsive iron-doped TiO2 and spontaneous sedimentation of the TiO2 particles.* Chemosphere, 2006. 65(11): p. 1976-1982.

[15] Sohrabi, S. and F. Akhlaghian, *Modeling and optimization of phenol degradation over copper-doped titanium dioxide photocatalyst using response surface methodology.* Process Safety and Environmental Protection, 2016. 99: p. 120-128.

[16] Di Paola, A., et al., *Preparation of Polycrystalline TiO2 Photocatalysts Impregnated with Various Transition Metal Ions: Characterization and Photocatalytic Activity for the Degradation of 4-Nitrophenol.* The Journal of Physical Chemistry B, 2002. 106(3): p. 637-645.